Supplementary Information

Hierarchical micro tiles growth of monoclinic tungsten oxide nucleated on MWCNTs hexagonal skeleton: Wide potential solid-state supercapacitor with mechanical bendable design

SI 1: Characterization

Crystal structure of obtained samples was studied with the help of RIGAKU X-ray diffractometer using Cu-Kα radiations of wavelength λ=1.5406 Å. Fourier transform infrared spectra (FTIR) were recorded by Thermofisher scientific iS50 in the wavenumber range 4000 to 400 cm^{-1}. The Raman studies were conducted using an excitation laser of 532 nm wavelength with NOST: HEDA-URSM4/5/7 Raman spectrometer. The UV-Visible absorbance spectra, ranging of 200 to 2400 nm wavelength were obtained using JASCO, V-770 double beam UV-Vis-NIR spectrophotometer. Chemical composition and states were scrutinized by X-ray photoelectron spectroscopy (XPS) through Thermo fischer k-Alpha X-Ray photoelectron spectrometer unit. ULTRA55 Field emission scanning electron microscopy (FE-SEM) (Karl Zeiss, MonoCI) was utilized to study surface morphology. For high resolution intrinsic morphological examination, transmission electron (300 kV FEG-TEM, FEI Tecnai G2, F30) microscopy was utilized. The electrochemical scrutiny such as cyclic voltammetry (CV), galvanostatic charge-discharge (GCD) and electrochemical impedance spectroscopy (EIS) of electrodes were conducted on PARSTAT-4000 potentiostat/galvanostat (Princeton Applied Research, USA), coupled with VersaStudio 2.10.01 software in the three electrodes configuration, with Ag/AgCl as reference electrode, deposited thin films as working electrode and platinum wire as counter electrode. Devices were tested in two electrode configuration by shortening counter and reference electrode to serve as one electrode. All electrochemical analysis was conducted at room temperature (27 ˚C)

SI 2: Materials

Multi-walled carbon nanotubes (MWCNTs) were obtained from Adnano technologies, while stainless steel (SS 304 grade, 46 gauge) was used as the substrate material. Sodium tungstate dihydrate (Na_2WO_4•$2H_2O$) (purity 98%), oxalic acid dihydrate ($C_2H_2O_4$•$2H_2O$) (purity 99.5%), 35% hydrochloric acid (HCl) were purchased from Merck and employed for synthesis of tungsten oxide. Lithium perchlorate ($LiClO_4$) (purity 95%) from Merck company served as electrolyte, and polyvinyl alcohol (PVA) (purity 94.3%) from LOBA Chemie company was used as gel polymer.

SI 3: Energy dispersive X-ray spectroscopy (EDAX)

Table SI3: Atomic percentage of C, W, and O of CWO2, CWO3, and CWO4.

Element	CWO2	CWO3	CWO4
C (At %)	77.51	57.19	67.73
W (At %)	0.71	3.30	1.61
O (At %)	21.78	39.51	30.67

SI 4: $W_{25}O_{73}$ micro-tile length and thickness studies

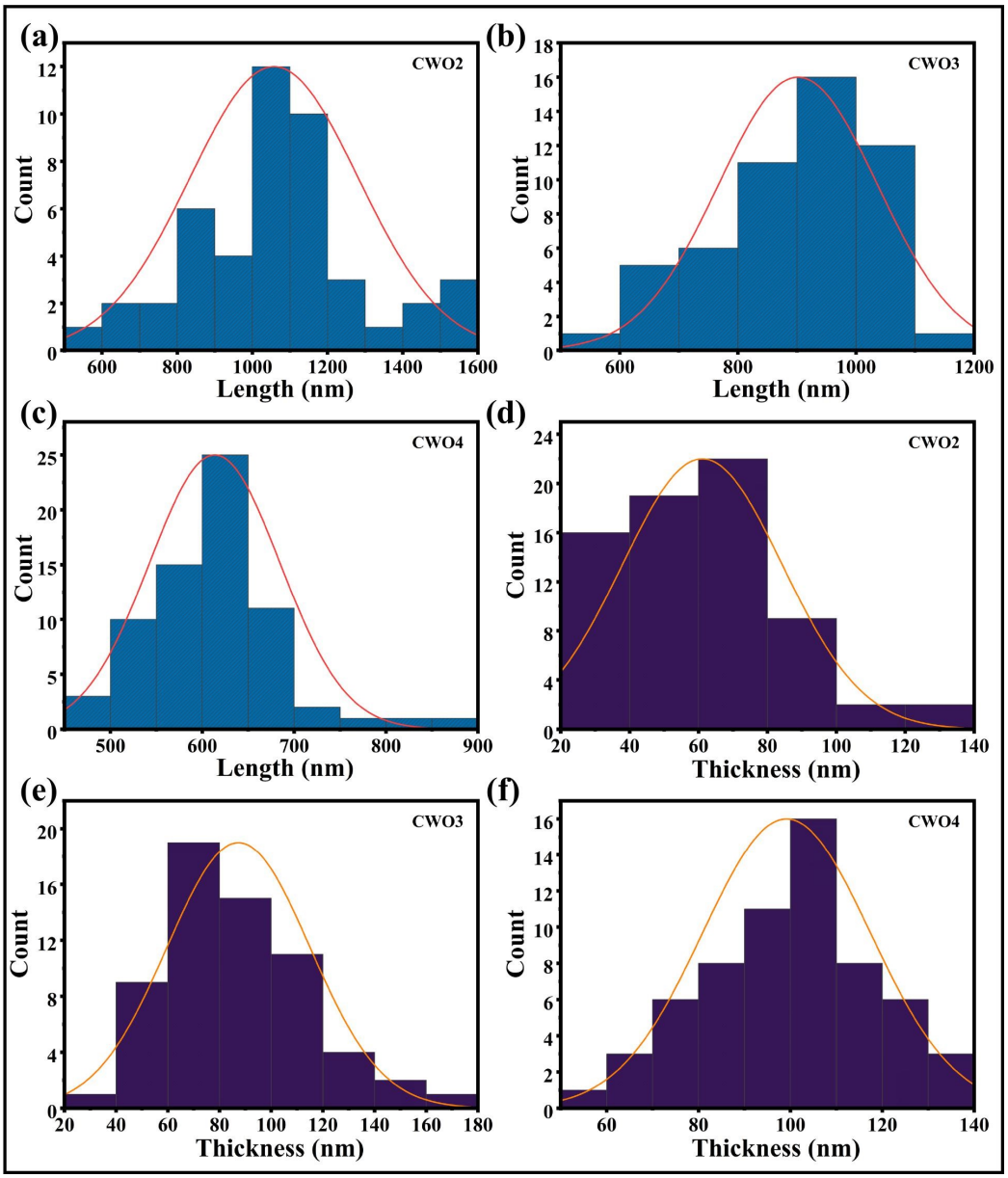

Figure S4: Histogram of $W_{25}O_{73}$ micro-tile length distribution of **(a)** CWO2, **(b)** CWO3, **(c)** CWO4, histogram of $W_{25}O_{73}$ micro-tile thickness distribution of **(d)** CWO2, **(e)** CWO3, and **(f)** CWO4.

SI 5: Electrochemical calculations

The specific capacitance was estimated through CV curves using the formula [1],

$$C_s = \frac{\int_i^f i(V)dV}{m.\Delta V.v} \quad \text{(SI-E-1)}$$

where, C_S specific capacitance (F/g), m is mass loading, ΔV is potential window and v is scan rate and integration term gives the area under CV voltammogram.

The specific capacitance, estimated through GCD curves with the help of following expression[1,2],

$$C_S = \frac{i\int_i^f Vdt}{m.\Delta V} \quad \text{(SI-E-2)}$$

Where i is applied current, $\int_i^f Vdt$ area under discharge curve, ΔV is potential window, m is mass loading.[3]

The energy density and power density of the flexible solid state supercaapcitor was calculated using the following formulas.

$$ED = \frac{1 C_s V^2}{2\ 3.6} \quad \text{(SI-E-3)}$$

Where, V is potential window, $C_s$is specific capacitance calculated using GCD.

$$PD = \frac{ED \bullet 3600}{\Delta t} \quad \text{(SI-E-4)}$$

SI 6: Effect of functionalization period on electrochemical performance

Fourier transform infrared spectroscopy

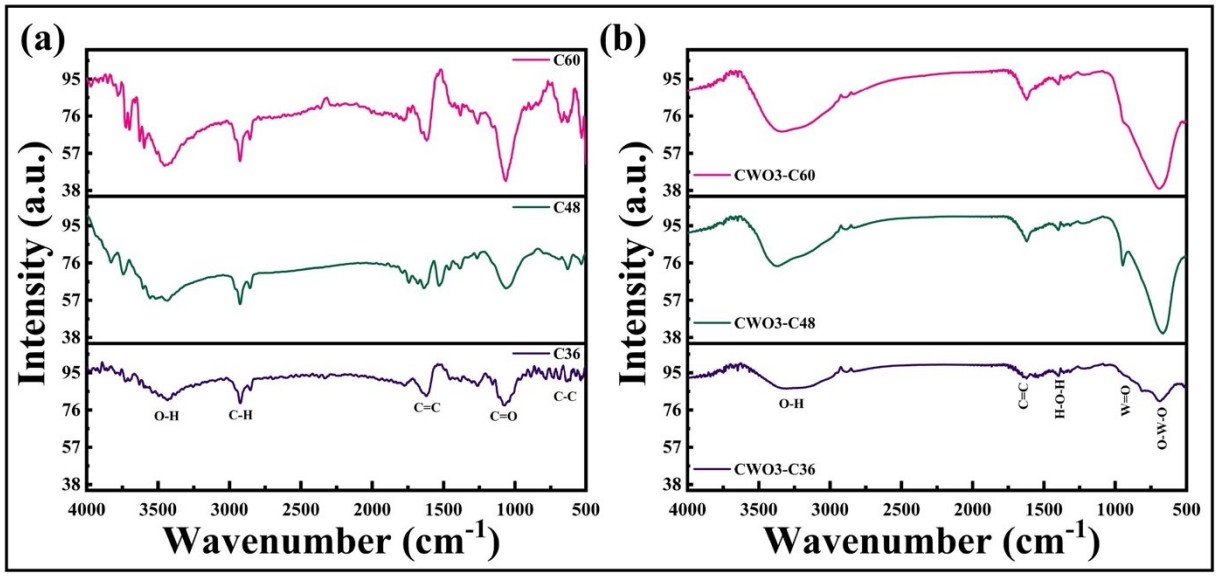

Figure S6 (a): FTIR spectra of **(a)** MWCNTs functionalized for 36, 48, 60 hr, and **(b)** CWO3 electrode with MWCNTs functionalized for 36, 48, 60 hr.

Fourier transform infrared (FTIR) spectra recorded for MWCNTs functionalized for 36, 48, and 60 hours are presented in figure S6 a (a). All the functionalized MWCNTs exhibited absorbance peaks corresponding to hydroxyl, and carboxyl groups along with C-C, and C=C associated with MWCNTs structure. FTIR showed broad peak around 3000 to 3500 cm^{-1} assigned to -OH groups. The peaks due to C-H, and C=O are present at 1072.23, and 2924.04 cm^{-1}, respectively. Peaks near 625.30, and 1622.32 arises due to C-C, and C=C vibrations. The FTIR spectra clearly shows the enhancement of absorbance peaks associated with functional groups (-OH, C-H, and C=O) with increase in functionalization time. Figure S6 a (b) shows the FTIR spectra of CWO3-C36, CWO3-C48 (CWO3), and CWO3-C60. All spectra exhibit characteristics absorption features within the wavenumber range of 400 to 4000 cm^{-1}, confirming the successful formation of MWCNTs-tungsten oxide composite. The vibrational bands observed at 694.73, and 956.51 cm^{-1}, are attributed to O-W-O bending and W=O stretching modes, respectively.[4] A distinct absorption peak positioned at 1622.32 cm^{-1} arises from the C=C stretching vibrations of MWCNTs.[5] The peak appearing at 1403.92 cm^{-1} corresponds to the H-O-H bending mode, indicating the presence of adsorbed water molecules.

While the broad absorption band spanning 3000 – 3500 cm^{-1} is associated with hydroxyl (-OH) groups in the composite.[5] The extent of functionalization can be clearly observed from the absorption peaks associated with -OH, and C=C groups.

Cyclic voltammetry

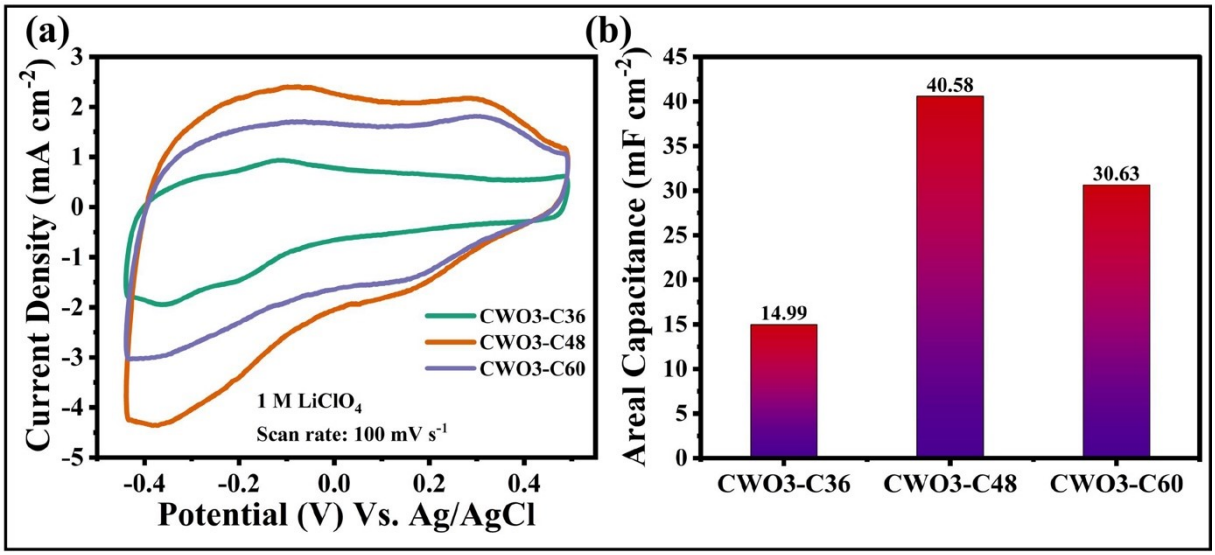

Figure S6 (b): (a) Cyclic voltammetry, and **(b)** areal capacitance of CWO3 electrode with MWCNTs functionalized for 36, 48, 60 hr.

The optimal ratio of functional groups (-COOH, and -OH) on MWNCTs, and tungsten oxide is very important as it affects the conductivity of electrode material. The cyclic voltammetry was performed for CWO3-C36, CWO3-C48, and CWO3-C60 (figure S6 b (a)). The CWO3-48 exhibited increased area under CV plot with distinct redox peaks in comparison

to CWO3-C36, and CWO3-C60. While CWO3-C36 showed near quasi rectangular shape with redox peaks. This might be due to significant contribution of MWCNTs in charge storage, with functional groups and deposited tungsten oxide helping in redox activities. With increasing the functionalization period to 60 hours in CWO3-C60, results in reduced conductivity, clearly depicted in CV curve. The calculated areal capacitance for CWO3-C36 (14.99 $mF \cdot cm^{-2}$), CWO3-C48 (40.58 $mF \cdot cm^{-2}$), and CWO3-C60 (30.63 $mF \cdot cm^{-2}$) at 100 $mV \cdot s^{-1}$ scan rate are depicted in figure S7 6 (b).

Electrochemical impedance spectroscopy

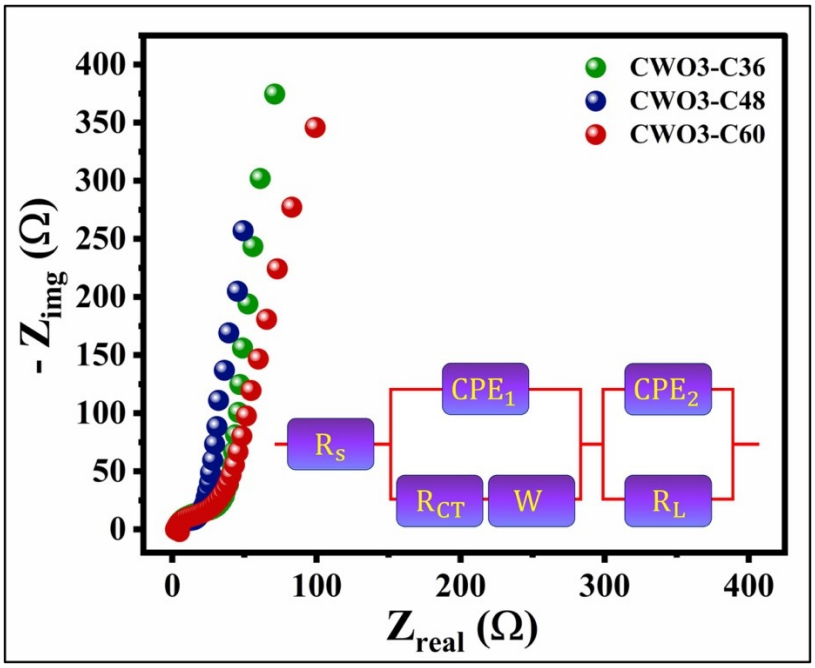

Figure S6 (c): Electrochemical impedance spectroscopy of CWO3 electrode with MWCNTs functionalized for 36, 48, 60 hr.

To study the resistive behavior of CWO3-C36, CWO3-C48, and CWO3-C60 electrochemical impedance spectroscopy was performed. Figure S6 (c) depicts the Nyquist plot of CWO3 with MWCNTs functionalized form 36, 48, and 60 hours. The solution resistance (

R_S) associated with ionic resistance of the electrolyte and electrical resistance of current collector, was found to be 2.56, 2.26, and 2.41 $\Omega \cdot cm^2$ for the CWO3 electrode with MWCNTs functionalization time of 36, 38, and 60 hr, respectively. The charge transfer resistance (R_{CT}) reflects how charge is transferred from electrolytic ion to external circuit. The CWO3-C48 exhibited low R_{CT} value of 16.28 $\Omega \cdot cm^2$ in comparison to CWO3-C36 (32.19 $\Omega \cdot cm^2$), and CWO3-C60 (23.21 $\Omega \cdot cm^2$). The low R_S, and R_{CT} values for CWO3-C48 is due to the optimum growth of tungsten oxide on MWCNTs facilitated by the functional groups. MWCNTs functionalized for 36 hours could not offer better electrochemical performance, this might be due to non-optimum growth of tungsten oxide. Whereas excessive functionalization (60 hr) might lead to reduced conductivity due to enhanced concentration of functional groups

Table SI6: R_s, and R_{CT} of CWO3 with MWCNTs functionalized for 36, 48, and 60 hr.

Parameters	CWO3-C36	CWO3-C48	CWO3-C60
R_S ($\Omega \cdot cm^2$)	2.56	2.29	2.41
R_{CT} ($\Omega \cdot cm^2$)	32.19	16.28	23.21

SI 7: Power law analysis

$$i = av^b \quad \text{(SI-E-5)}$$

where, v is the scan rate, i represents current density, a and b, are variables.

SI 8: Differential Trasitti model

$$Q_t = Q_s + Q_d \quad \text{(SI-E-6)}$$

$$Q_d \, \alpha \, v^{-0.5} \quad \text{(SI-E-7)}$$

SI 9: Dunn method

$$i = k_1 v + k_2 v^{0.5} \quad \text{(SI-E-8)}$$

$$\frac{i}{v^{0.5}} = k_1 v^{0.5} + k_2 \quad \text{(SI-E-9)}$$

Where k_1, and k_2 are the constants correlated to surface capacitive, and diffusion-controlled mechanisms respectively.

SI 10: Mott-Schottky

$$\frac{1}{C^2} = \left[\frac{2}{e\varepsilon\varepsilon_0 N_d A^2}\right] \cdot \left[E - E_{fb} - \frac{KT}{e}\right] \quad \text{(SI-E-10)}$$

Where, C corresponds to capacitance, e_0 represents charge of electron, **ε**, and ε_0 stands for permittivity of material and vacuum respectively, N_d is electron donor density. The E, and E_{fb} are applied and flat band potentials respectively [6]. The E_{fb} is determined by extrapolating the fitted line to $C^{-2} = 0$.

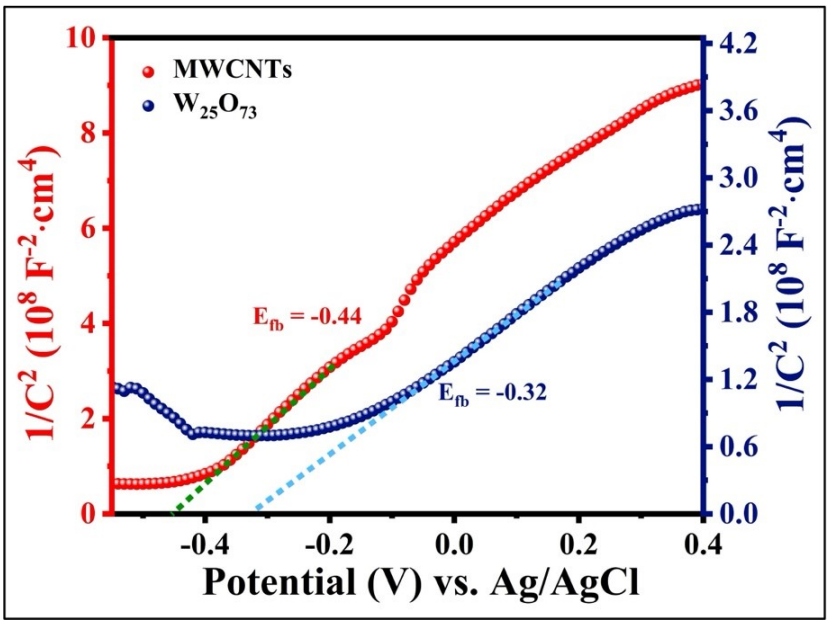

Figure S10: Mott-Schottky plot for MWCNTs, and $W_{25}O_{73}$.

SI 11: Galvanostatic charge discharge studies of SS, MWCNTs, WO3, and CWO3

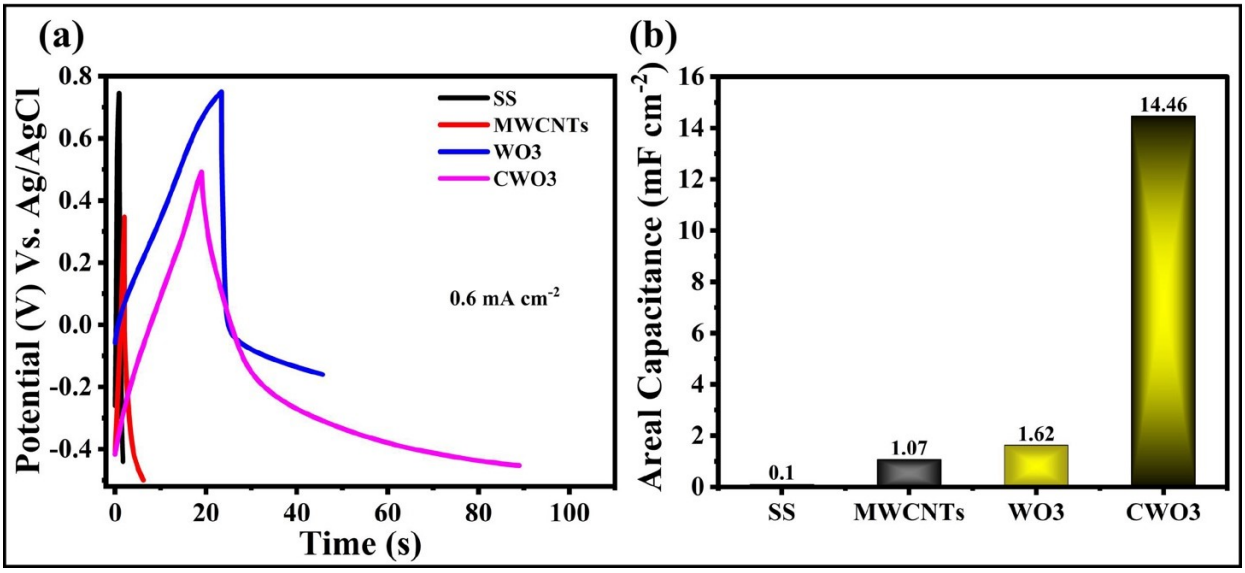

Figure S11: (a) Galvanostatic charge discharge, and **(b)** areal capacitance of SS, MWCNTs, WO3, and CWO3.

SI 12: Impedance of constant phase element:

$$Z_{CPE} = \frac{1}{T(j\omega)^n} \qquad \text{(SI-E-11)}$$

where, T and n, represents the frequency independent terms and gives the angular frequency. The varies in the range of -1 to +1, for ideal capacitor its value is found to be 1, whereas for inductor its value is -1. For resistive circuit, its value present in the range of 0 to 0.5.[7]

SI 13: Diffusion coefficient

$$D = 0.5\,(\frac{RT}{AF^2\sigma_\omega C})^2 \qquad \text{(SI-E-12)}$$

Where R (8.314 $J.mol^{-1}.K^{-1}$) is gas constant, T (300 K) is room temperature, F (96500 $C.mol^{-1}$) is Faraday's constant, A (1 × 1 cm^2) implies area of the electrode, C indicates molar concentration of Li^+ ions, and σ_w represents the Warburg diffusion. Slope of the plot real impedance versus $\omega^{-1/2}$.[8]

SI 14: Electrochemical stability analysis of CWO3 electrode

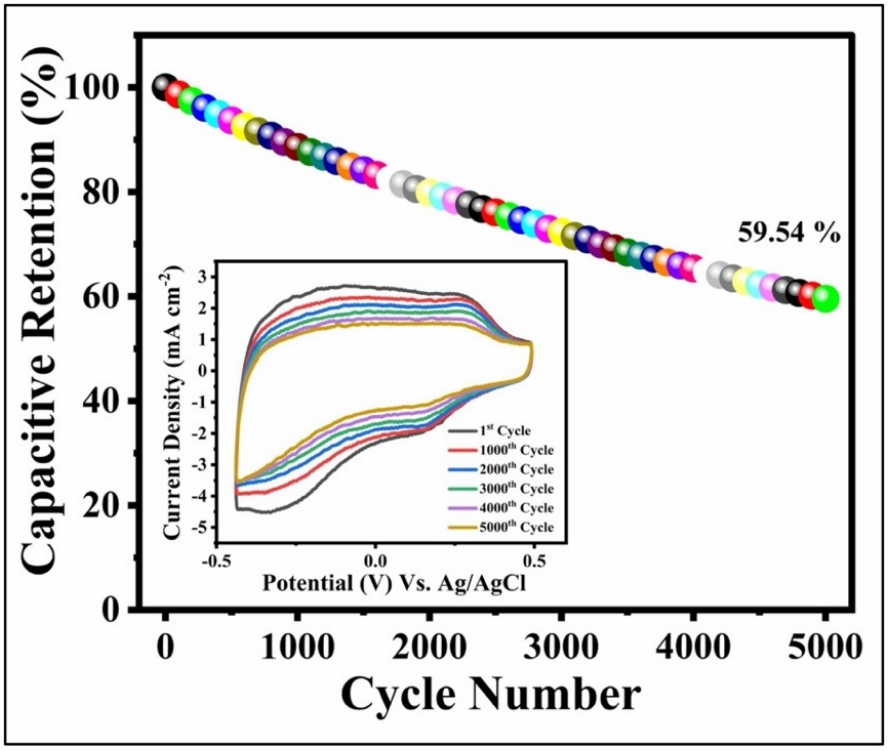

Figure S14: Electrochemical stability analysis of CWO3 for 5000 CV cycles.

SI 15: Structural, morphological, elemental, and electrochemical impedance analysis of CWO3 electrode after stability analysis.

X-ray diffraction:

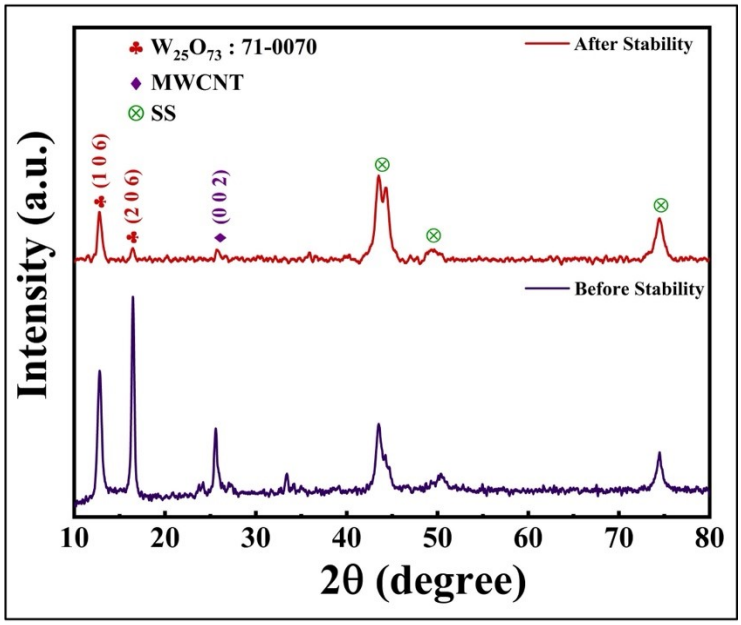

Figure S15 (a): X-ray diffraction analysis of CWO3 before and after electrochemical stability.

Field emission scanning electron microscope:

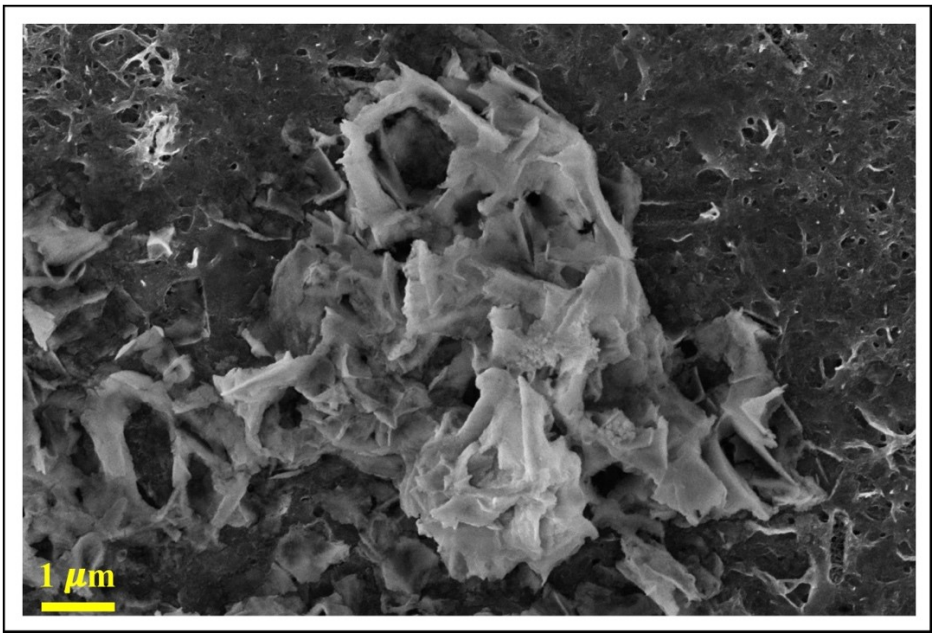

Figure S15 (b): FE-SEM micrograph of CWO3 after electrochemical stability.

Energy dispersive X-ray spectroscopy (EDAX):

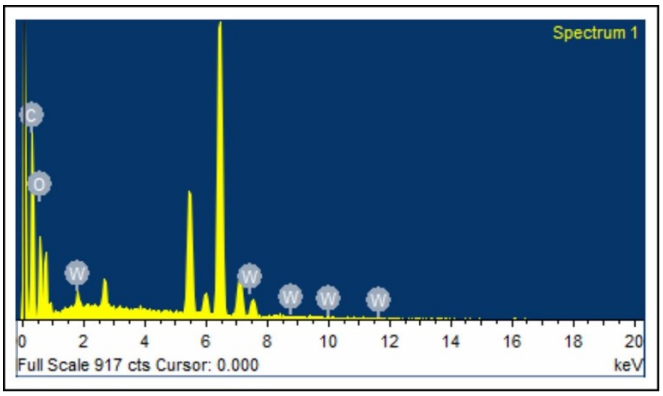

Figure S15 (c):EDAX analysis of CWO3 after electrochemical stability.

Table SI15 (a): Atomic percentage of C, W, and O in CWO3 electrode before and after stability.

Element	Before stability	After stability
C (At %)	57.19	64.37
W (At %)	3.30	0.18
O (At %)	39.51	35.45

Electrochemical impedance spectroscopy:

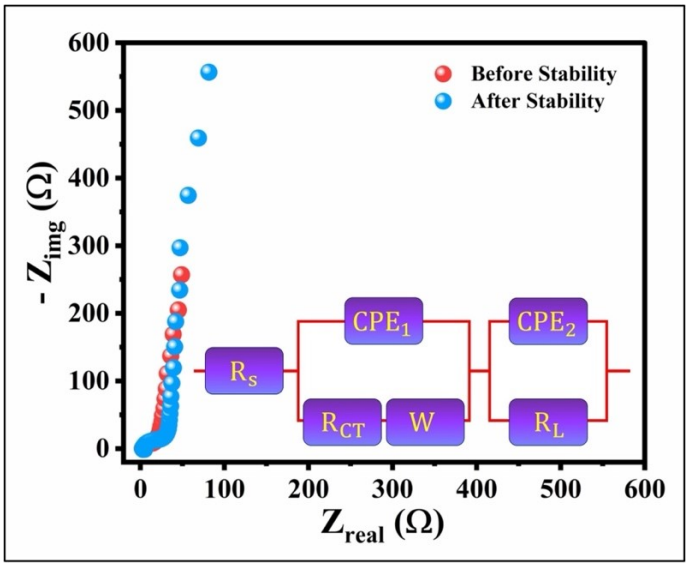

Figure S15 (d): Electrochemical impedance spectroscopy of CWO3 before, and after electrochemical stability.

Table SI15 (b): R_s, and R_{CT} of CWO3 before, and after electrochemical stability.

Parameters	Before stability	After Stability
R_S $(\Omega \cdot cm^2)$	2.29	2.9
R_{CT} $(\Omega \cdot cm^2)$	16.28	25.47

SI 16: Mechanical flexibility studies of symmetric solid-state device after electrochemical stability analysis

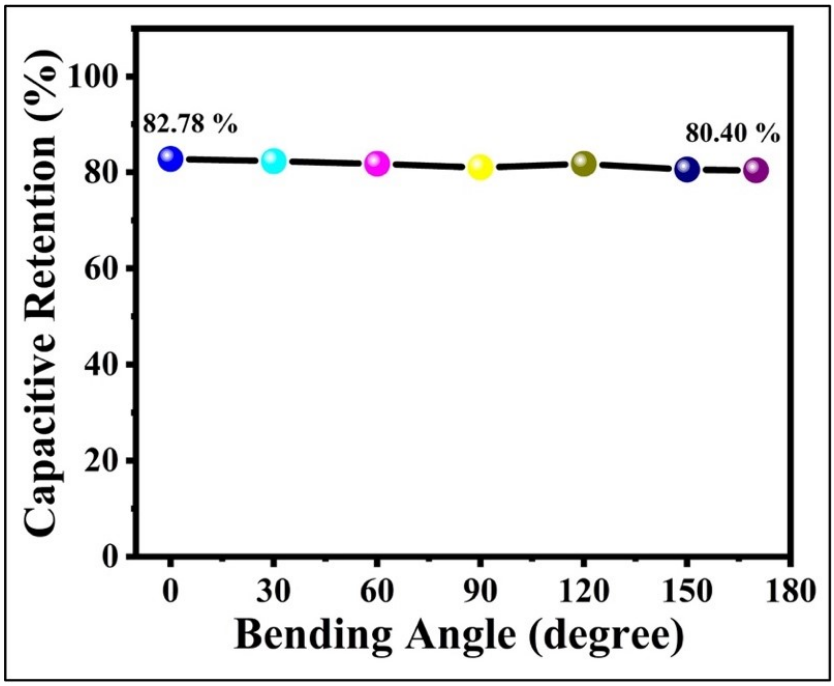

Figure S16: Capacitive retention under different bending angle for symmetric solid-state device after electrochemical stability analysis.

SI 17: Mass loading of MWCNTs,

Table SI 17: Mass loading of MWCNTs, $W_{25}O_{73}$, and MWCNTs/$W_{25}O_{73}$

Sample	MWCNTs	$W_{25}O_{73}$	MWCNTs/ $W_{25}O_{73}$
CWO2	0.04 mg	0.15	0.19 mg
CWO3	0.04 mg	0.17	0.21 mg
CWO4	0.04 mg	0.16	0.20 mg

References:

1 A. Agarwal and B. R. Sankapal, *J Mater Chem A Mater*, 2021, 9, 20241–20276.

2 W. Cheng, W. Huang, A. Zhang, Y. Du, L. Cui, P. Tian and J. Liu, *ChemElectroChem*, DOI:10.1002/celc.202201051.

3 D. Gandla, X. Wu, F. Zhang, C. Wu and D. Q. Tan, *ACS Omega*, 2021, 6, 7615–7625.

4 S. O. Ogungbesan, O. Ejeromedoghene, Y. Moglie, E. Buxaderas, B. Cui, R. A. Adedokun, M. Kalulu, M. A. Idowu, D. Díaz Díaz and G. Fu, *New Journal of Chemistry*, 2024, 48, 15428–15435.

5 D. Park, H. Ju, T. Oh and J. Kim, *RSC Adv*, 2018, 8, 8739–8746.

6 Interpretation of Mott–Schottky plots of photoanodes for water splitting - Chemical Science (RSC Publishing) DOI:10.1039/D1SC06401K, https://pubs.rsc.org/en/content/articlehtml/2022/sc/d1sc06401k, (accessed 25 December 2025).

7 J. Zhang and X. S. Zhao, *ChemSusChem*, 2012, 5, 818–841.

8 P. Xiao, Y. Cai, X. Chen, Z. Sheng and C. Chang, *RSC Adv*, 2017, 7, 31558–31566.